




Dodecyltrimethylammonium bromide surfactant effects on DNA: Unraveling the competition between electrostatic and hydrophobic interactions

E. F. Silva


Departamento de Física, Universidade Federal de Viçosa, Viçosa, Minas Gerais, 36570-900, Brazil
and Departamento de Física, Universidade Federal de Juiz de Fora, Juiz de Fora, Minas Gerais, 36036-900, Brazil

U. M. S. Andrade

Departamento de Física, Universidade Federal de Viçosa, Viçosa, Minas Gerais, 36570-900, Brazil
and Departamento de Formação Geral, Centro Federal de Educação Tecnológica de Minas Gerais, Curvelo, Minas Gerais, 35790-000, Brasil

K. M. de Oliveira , A. V. N. C. Teixeira , and M. S. Rocha *

Departamento de Física, Universidade Federal de Viçosa, Viçosa, Minas Gerais, 36570-900, Brazil

 (Received 20 April 2020; revised 1 July 2020; accepted 16 August 2020; published 1 September 2020)

We present a new study on the interaction of the DNA molecule with the surfactant dodecyltrimethylammonium bromide (DTAB), performed mainly with optical tweezers. Single-molecule force spectroscopy experiments performed in the low-force entropic regime allowed a robust characterization of the DNA-DTAB interaction, unveiling how the surfactant changes the mechanical properties of the biopolymer, the binding parameters, and the competition of the two mechanisms involved in the interaction: electrostatic attraction between the cationic surfactant heads and the negative phosphate backbone of the DNA and hydrophobic interactions between the tails of the bound DTAB molecules, which can result in DNA compaction in solution depending on the quantity of bound surfactant. Finally, force clamp experiments with magnetic tweezers and gel electrophoresis assays confirm that DTAB compacts DNA depending not only on the surfactant concentration but also on the conformation of the biopolymer in solution. The present study provides new insights on general aspects of the DNA-surfactant complexes formation, contributing to the fundamental knowledge of the physics of such interactions.

DOI: [10.1103/PhysRevE.102.032401](https://doi.org/10.1103/PhysRevE.102.032401)

I. INTRODUCTION

Surfactants are amphiphilic molecules that play important roles in industrial processes, acting as detergents, emulsifiers, dispersants, or foaming and wetting agents. These molecules have two distinct parts, a hydrophilic head and a hydrophobic tail, and due to this amphiphilic feature, surfactants tend to stay at interfaces, reducing the surface tension at a liquid-liquid, a liquid-air, or a liquid-solid interface. In solution, surfactants also have the tendency to form micelles above a certain concentration [critical micelle concentration (CMC)] in order to avoid the contact of their hydrophobic tails with water, minimizing the free energy of the system at this configuration.

In the past few years, interactions between polyelectrolytes and oppositely charged surfactants have been extensively studied. It is well established that, at low surfactant concentrations, the driving force of such associations is the electrostatic attraction between the polyelectrolytes and the surfactant molecules. For high surfactant concentrations, on the other hand, the binding usually results in a phase separation due to the strong cooperative behavior of hydrophobic interactions

that start to dominate the binding process at such concentrations [1]. Thus, from the point of view of fundamental physics, the interactions between surfactants and polyelectrolytes is a very rich field due to the amphiphilic nature of surfactants, which can lead to a competition between very different binding modes. Such competition motivates the investigation of possible transitions between the different modes, the evaluation of the relative magnitudes between the interactions behind these modes, and the search of conditions in which this relative magnitude can be modulated by solution properties like the surfactant concentration, ionic strength, pH, and/or the type of counterions used; see for example, Ref. [1].

In particular, much attention has been given to the interactions of surfactants with biological relevant macromolecules, and in particular with DNA, a negatively charged biological polyelectrolyte [2–13]. This kind of study is important not only to test the toxicity of industrial surfactants but also because they can bring new useful information for the application of these molecules in fields such as the control of DNA compaction and decompaction [14,15], nucleic acids purification [16], drug delivery [9], gene therapy [6,7,17], gene expression [18], and in the development of biosensors [19].

In the present work we report a study on the DNA interaction with the surfactant dodecyltrimethylammonium bromide (DTAB), performed at the single-molecule level. We were

*marcios.rocha@ufv.br

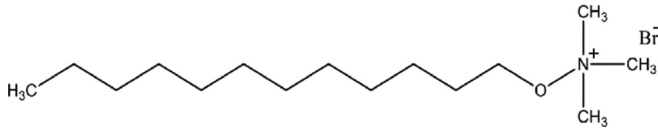


FIG. 1. Chemical structure of the DTAB surfactant.

able to identify and characterize in detail the two different components of the binding mechanism: electrostatic attraction between the cationic head of DTAB and the negative phosphate backbone of the DNA double helix, followed by a strong hydrophobic interaction between the tails of the bound DTAB molecules, resulting in a DNA compaction induced by the surfactant. Although there is a previous study in the literature which uses optical tweezers to perform force spectroscopy with DNA-DTAB complexes, such a study was performed in the high-force enthalpic regime, in which the complexes are stretched with forces on the order of tens of piconewtons [4]. On the contrary, our study uses very low forces ($\lesssim 3$ pN) to stretch the complexes, i.e., we work in the entropic regime, where the forces are small enough to only change the biopolymer conformation in solution, not affecting its structure. Such regimes give completely different insights on different aspects of the interaction; while the former is useful to understand the changes on the DNA secondary structure and helix stability on surfactant binding, the latter gives insights on the mechanical properties of the complexes formed and on the physical chemistry of the interaction [20–22]. Finally, note that the approach presented here can contribute to improving the fundamental knowledge about DNA-surfactant systems and possibly to the development of novel applications for these complexes.

II. MATERIALS AND METHODS

DTAB was purchased from Sigma-Aldrich and used without further purification. Figure 1 shows the chemical structure of this surfactant.

All experiments with DNA were performed in a phosphate-buffered saline (PBS) solution whose composition is as follows: $[\text{Na}_2\text{HPO}_4] = 4.375$ mM, $[\text{NaH}_2\text{PO}_4] = 1.25$ mM, and $[\text{NaCl}] = 140$ mM, pH 7.4, and ionic strength $I = 154$ mM.

A. Electrical conductivity and CMC determination

Before investigating the DTAB association to DNA it is fundamental to determine the CMC concentration of the surfactant in pure solvent in order to know whether micelles are formed in solution under our experimental conditions and to evaluate the role of DNA on micelle formation in our interaction experiments.

Here we have determined the CMC of DTAB by measuring the electrical conductivity of the solution (surfactant + solvent) with a conventional conductivity meter (DIGIMED DM-32), where injections of $40 \mu\text{l}$ from a concentrated solution of DTAB (50 mM) were added to 20 ml of water. The solution was stirred for 60 s after each injection to reassure that the equilibrium was reached. The same experiment was also performed using our PBS buffer instead of water, such

that the CMC could be determined in the solvent used in the interaction experiments.

B. Optical tweezers

For optical tweezers assays, the sample chamber consists of an o-ring glued in a streptavidin-coated coverslip, where the working solution is deposited. This solution contains λ -DNA molecules ($\sim 48,500$ base pairs, $\sim 16.5 \mu\text{m}$ contour length, Promega Corp. D1501) end labeled with biotin. One end of the molecules is attached to a streptavidin-coated polystyrene bead, $3.0 \mu\text{m}$ in diameter (Bangs Labs), while the other end is attached to a streptavidin-coated coverslip. With this procedure, the DNA molecules became tethered by the ends between the bead and the coverslip. DNA and DTAB were incubated for ~ 20 min for surfactant equilibration before starting the measurements.

The optical tweezers used consist of a 1064-nm fiber laser (IPG Photonics) mounted in a Nikon Ti-S inverted microscope with a $100\times$ N.A. 1.4 objective (a single-beam optical tweezer).

The DNA molecules and the DNA-DTAB complexes are stretched using a piezoelectric device (Physik Instrumente) to move the microscope stage. The force-extension curves (FECs) collected were fitted to the Marko-Siggia equation of the wormlike chain (WLC) model [23] using a standard procedure [24]. From these fittings, the mechanical parameters (contour and persistence lengths) were determined with high accuracy for various different DTAB concentrations. The reported values of these parameters and the corresponding error bars (standard error of the mean) were obtained for each DTAB concentration using eight different DNA molecules, performing six force-extension curves for each different molecule. We limit the maximum stretching forces to ~ 3 pN, therefore working within the entropic regime, as stated earlier. This is important for determining the mechanical properties with accuracy and guarantees that the system is always close to the chemical equilibrium [21]. In addition, this is the regime that allows one to measure the “apparent contour length” resulting from DNA compaction, since high stretching forces decompact collapsed DNA [21,25,26]. Here we call this “apparent contour length” just contour length, since all our experiments are restricted to the entropic regime. Complete details of our experimental procedures used with this technique can be found in a previous work [24].

C. Magnetic tweezers

The sample preparation procedure for the magnetic tweezers experiments is very similar to that used for optical tweezers; the main difference is that here we use streptavidin-coated superparamagnetic beads, $2.8 \mu\text{m}$ in diameter (Invitrogen M-280), for DNA attachment.

The magnetic tweezers used here is mounted in a Nikon Ti-S inverted microscope with a $100\times$ N.A. 1.3 objective. A homemade three-dimensional stage to control the position of a permanent magnet with precision is mounted above the microscope objective using three Newport linear stages (UMR5.25) and a piezoelectric device (Newport PZA12). With this apparatus, one can align the magnet position with

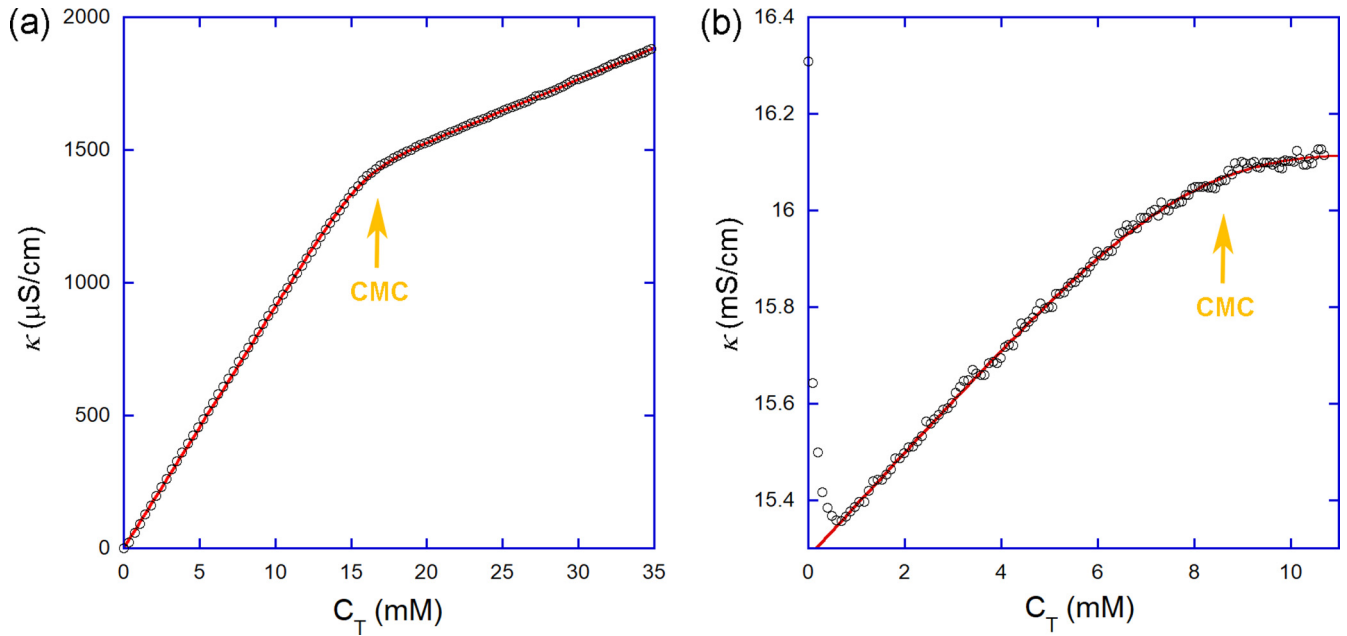


FIG. 2. Electrical conductivity κ of DTAB solutions in (a) water and (b) PBS. From these curves we determine the CMC of the surfactant in each solvent. The arrows indicate the CMC in each curve: (15.7 ± 1.1) mM in water and (8.1 ± 1.4) mM in PBS.

the sample chamber to apply forces to the superparamagnetic beads and, consequently, to the tethered DNA molecules.

The DNA molecules are stretched along the optical axis of the microscope (i.e., perpendicularly to the coverlip surface) with a certain desired constant force by positioning the magnet adequately. DNA extension was obtained by determining the bead height relative to the coverslip surface. Such measurements is done with a standard calibration procedure in which we compare the contrast on the center of the working bead (attached to DNA) with the contrast on the center of an identical bead glued on the coverlip surface, whose height is known to be equal to the bead radius. Such a procedure is similar to others used in the literature to determine the DNA extension in magnetic tweezers experiments [27,28]. The force applied on DNA is determined by analyzing the bead fluctuations, a standard procedure also used in previous works [27,28]. The error bars (standard error of the mean) reported in the results refer to different measurements performed over the same DNA molecule.

D. Gel electrophoresis

In order to confirm the DTAB-induced DNA compaction with a bulk technique, we have performed gel electrophoresis assays incubating DTAB with DNA at various concentrations of the surfactant in an agarose gel (1.2% in mass), maintaining the DNA concentration fixed, as performed in our force spectroscopy experiments.

The experiments were performed following a procedure similar to the assays of Murphy and Zimmerman [29]. First, DNA and DTAB were incubated in a microtube at desired concentrations for a few hours. Then, the microtubes were centrifuged at 14,000 rpm for 30 min, and the supernatant is then separated from the rest of the sample, which is discarded. The compacted DNA molecules tend to sink, staying

at the bottom of the microtube after centrifugation. Thus, it is expected that the supernatant will contain more DNA for low DTAB concentrations, when the compaction induced by the surfactant is lesser.

III. RESULTS AND DISCUSSION

A. CMC determination

The results showing the solution conductivity as a function of the DTAB concentration in solution are shown in Fig. 2 for [Fig. 2(a)] deionized water and [Fig. 2(b)] PBS. The CMC is determined with a method previously described [30], and the results obtained were (15.7 ± 1.1) mM in water and (8.1 ± 1.4) mM in PBS. These results are compatible to those found by other groups [31].

B. Force spectroscopy with optical tweezers allows the unveiling of the different binding mechanisms involved in the DNA-DTAB interaction

In Fig. 3 we show some exemplifying FECs for some DTAB concentrations. The WLC fittings are also shown as solid lines. Observe that the WLC model fits very well to our experimental data, allowing the determination of the contour and persistence lengths with accuracy. Observe that the FEC corresponding to 0.2 mM of DTAB (blue squares) is very close to the bare DNA curve (red circles), indicating that the mechanical parameters of the DNA-DTAB complexes vary little within this concentration range. On the other hand, the FEC measured for 0.4 mM of DTAB (green diamonds) is very different, which indicates that substantial changes on the mechanical properties, especially on the apparent DNA contour length, occurs at such a concentration.

The FECs along with the mechanical properties derived from the fittings are the raw results determined from our force

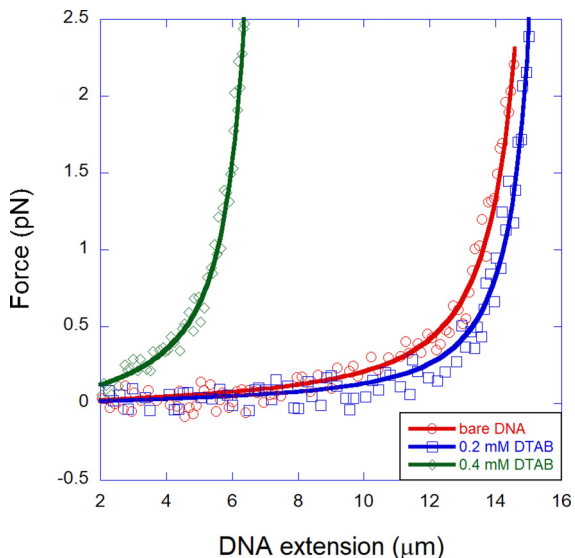


FIG. 3. Force-extension curves (FECs) obtained for some DTAB concentrations. The solid lines are fittings to the WLC model, from which the mechanical parameters of the complexes are extracted.

spectroscopy measurements performed with optical tweezers, free of any interpretation. The mechanical properties are shown in Figs. 4 and 5.

In Fig. 4 we show the contour length L of the complexes formed between DNA and DTAB as a function of the surfactant concentration in the sample C_T . Observe that this mechanical parameter stays constant until $C_T \sim 0.35$ mM and then abruptly decreases, indicating that DTAB strongly compacts DNA above a certain critical concentration, which for our

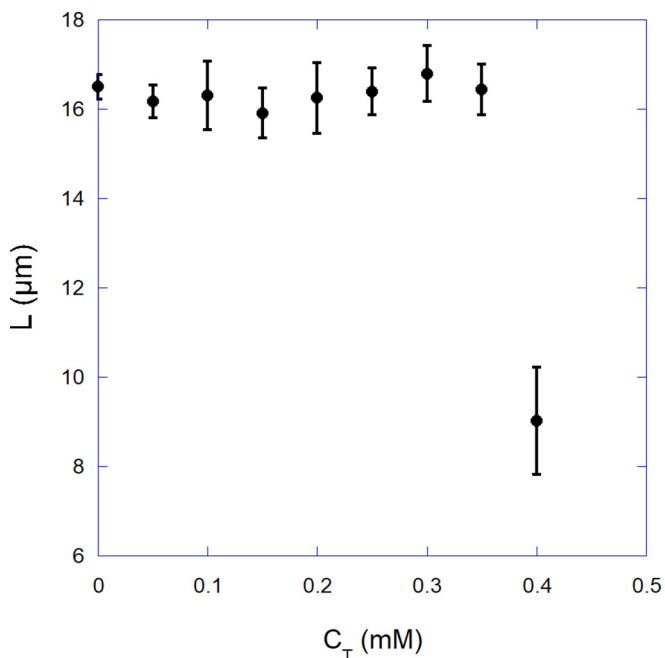


FIG. 4. Contour length L of the DNA-DTAB complexes as a function of the surfactant concentration in the sample C_T . Observe that the contour length remains constant until a certain critical concentration, $C_T \sim 0.35$ mM, and then abruptly decreases.

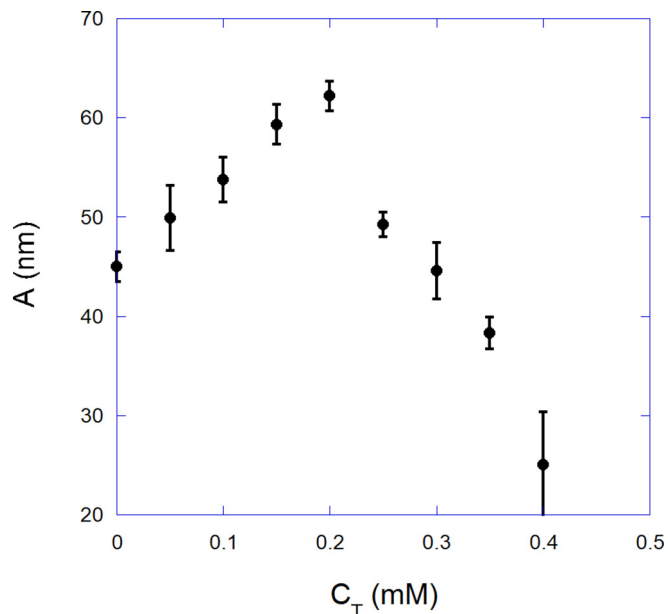


FIG. 5. Persistence length A of the DNA-DTAB complexes as a function of the surfactant concentration in the sample C_T . One can distinguish two distinct behaviors: For low concentrations ($C_T < 0.2$ mM) the persistence length increases as DTAB binds to the double helix. For $C_T > 0.2$ mM, the mechanical parameter strongly decreases. This behavior suggest that two different binding mechanisms play a role here.

experimental conditions is between 0.35 and 0.40 mM. It is very difficult to obtain more experimental data of the mechanical properties beyond this critical concentration, since DNA compaction induced by the surfactant tends to bring the bead attached to the DNA very close to the coverslip surface, often attaching such bead on the surface (which ends the experiment).

This abrupt DNA compaction measured here resembles somewhat the DNA condensation process induced by multivalent cations. In such a process, cations with charge equal or higher than $+3$ condense DNA into tiny globules, toroids, or other structures above a certain critical concentration, and the condensation occurs in a very narrow ligand concentration range [32–34], resembling a high cooperative “none-or-all” process [35,36]. When using multivalent cations, the condensation is a result of a high neutralization of the DNA negative phosphate backbone. In the present case, however, there is a noticeable difference: The hydrophobic interactions between the surfactant tails is the driven force that promotes DNA compaction, as will be evidenced below, since the positive head of DTAB is monocationic and thus have a limited electrostatic effect in neutralizing the DNA phosphate backbone.

In Fig. 5 we show the corresponding persistence length A of the same DNA-DTAB complexes as a function of the surfactant concentration in the sample C_T . Here one can clearly distinguish two distinct behaviors: For low concentrations ($C_T < 0.2$ mM) this mechanical parameter increases as DTAB binds to the double helix. For $C_T > 0.2$ mM, on the other hand, it strongly decreases. Such data suggest that two different binding mechanisms play a role here, the first one

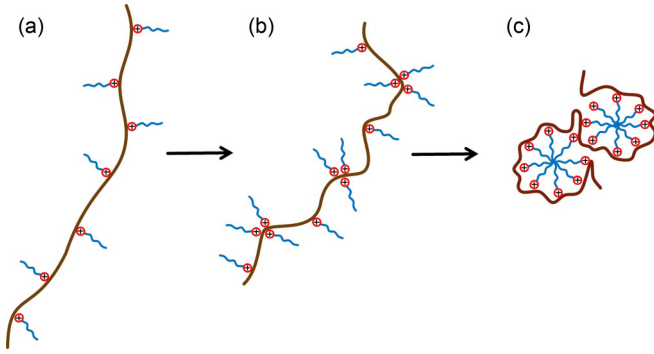


FIG. 6. Scheme of the DNA-DTAB interaction, showing three different steps of the binding mechanism. (a) At low surfactant concentrations, DTAB molecules bind individually along the double helix, and such binding is initially driven by the electrostatic interaction between the positive surfactant heads and the negative phosphate backbone of the double helix, although the hydrophobic tails play a role in the resulting persistence length. (b) As the DTAB concentration reaches a certain threshold, the hydrophobic interactions between the tails of the surfactant molecules start to dominate the binding process. (c) When there are sufficient DTAB molecules very close to each other, they can form a structure similar to a micelle, compacting the DNA molecule.

increasing the persistence length and the second one decreasing this parameter until finally inducing the compaction of the biopolymer.

Based on the data of Figs. 4 and 5 we propose the following scenario for the DNA-DTAB interaction. A illustrating scheme is shown in Fig. 6 to help in the following discussion. It is known that surfactants in general interact with DNA via a competition of electrostatic and hydrophobic interactions [4,10] and that some surfactants can compact DNA depending on the size of the hydrophobic tail [4,12]. First, at low surfactant concentrations, DTAB molecules bind individually along the double helix, as represented in Fig. 6(a). Such interaction is mediated initially by the electrostatic attraction between the positive surfactant head and the negative phosphate backbone of the double helix. Observe, however, that even here the hydrophobic tail plays a role on the mechanics of the resulting complex, since the persistence length increases for low DTAB concentrations—a behavior opposite to that expected if the interaction involved only phosphate charge neutralization [37,38]. Thus we propose that DTAB molecules bind individually for $C_T < 0.2$ mM, as shown in Fig. 6(a). When the DTAB concentration reaches a certain threshold, the hydrophobic tails tend to stay close in order to avoid contact with surrounding water, and the hydrophobic interactions between those tails start to dominate the binding process: As more DTAB molecules bind to double helix, there is a preference for these molecules to bind very close to the previously bound DTAB due to the hydrophobic interaction between their tails, maximizing the entropy of the system. Such situation is illustrated in Fig. 6(b) and approximately corresponds to the concentration range $0.2 \text{ mM} < C_T < 0.4 \text{ mM}$, in which the contour length remains constant but the persistence length decreases due to bendings introduced on DNA as a result of the surfactant aggregation. Finally, when there are sufficient

DTAB molecules very close to each other, they can form a structure similar to a micelle, as illustrated in Fig. 6(c), compacting the DNA molecule. For our experimental conditions, such behavior starts to occur at $C_T \sim 0.4$ mM and can explain the abrupt decrease measured for the DNA contour length at this concentration (see Fig. 4). We note that such micelle-type aggregation occurs at a concentration much smaller than the DTAB CMC, which was measured here as ~ 8.1 mM in PBS. Thus, note that micelle formation is highly facilitated along the DNA, i.e., the biopolymer promotes the aggregation of bound surfactant molecules in a micelle-type structure. Such behavior is expected, since the surfactant molecules bound to DNA tend to stay, on average, closer to each other than when they are free in solution. Note that there are two different transitions on the DNA-DTAB system. The first one occurs at $C_T \sim 0.2$ mM, where hydrophobic interactions between the surfactant tails start to strongly dominate the binding process inducing the decrease of the persistence length. The second transition, on the other hand, takes place at $C_T \sim 0.4$ mM, with the formation of the micelle-type structures that results in DNA compaction.

In order to advance in the above discussion, we use a quenched-disorder statistical model of ligand binding developed by our group [21,39] to extract the physical chemistry of the DNA-DTAB interaction from the persistence length data of Fig. 5. Such modeling was discussed in detail in a previous review article [21]. Here we propose that two different binding isotherms can be used to describe the two different binding mechanisms presented in Figs 5 and 6: A first binding isotherm (BI 1) describes the individual DTAB binding in the low concentration range (0 to 0.2 mM of DTAB) and a second binding isotherm (BI 2) describes the mechanism dominated by the hydrophobic interactions between the surfactant tails, which occurs in the high concentration range (0.2 to 0.4 mM of DTAB).

We choose the Hill equation as the binding isotherms to perform the fittings. Such an equation reads

$$\frac{r}{r_{\max}} = \frac{(KC_f)^n}{1 + (KC_f)^n}, \quad (1)$$

where r is the bound site fraction (fraction of DNA base pairs occupied by the bound ligands), r_{\max} is the saturation value of r , K is the equilibrium association binding constant, C_f is the free (not bound to DNA) ligand concentration, and n is the Hill exponent, a parameter that measures the cooperativity degree of binding reactions [21].

Such an isotherm can be plugged into our model that predicts how the persistence length varies as the ligand molecules bound to the double helix,

$$\frac{1}{A} = \frac{1 - r/r_{\max}}{A_0} + \frac{r/r_{\max}}{A_1}, \quad (2)$$

where A_0 is the persistence length of the bare DNA molecule and A_1 is the local persistence length induced by the ligand on binding on a site (or, equivalently, the persistence length at bound ligand saturation).

The model was used to fit the experimental data of Fig. 5 and the results are shown in Fig. 7. Observe that each binding isotherm (BI 1 and BI 2, each with a different set of binding parameters) fits well to the experimental data, and from these

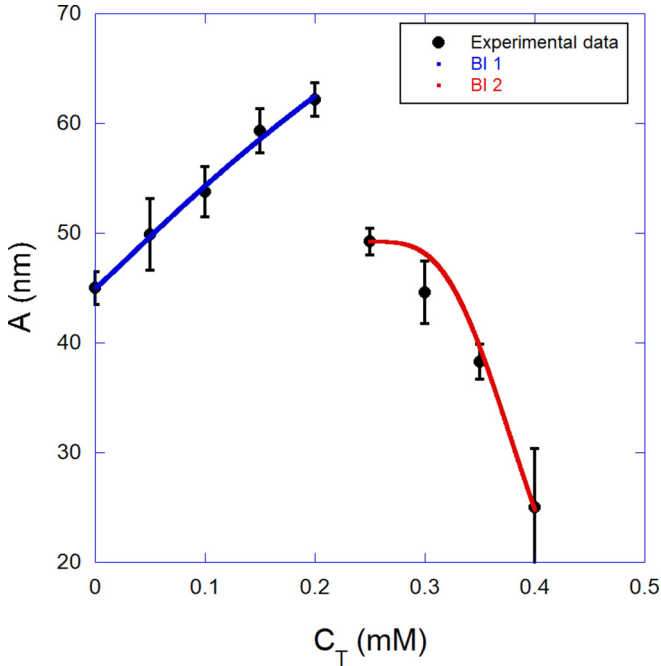


FIG. 7. Fittings of the persistence length data performed with our quenched-disorder statistical model of ligand binding [21,39], from where the binding parameters were determined. Two different binding isotherms were used to describe the different binding mechanisms: individual DTAB binding at the low concentration range (0 to 0.2 mM of DTAB) and the mechanism dominated by the hydrophobic interactions between the surfactant tails, which occurs in the high concentration range (0.2 to 0.4 mM of DTAB).

fittings we determine the binding parameters shown in Table I. One should note in Fig. 7 that extrapolating the two proposed binding isotherms does not allow them to cross each other. This fact is because such proposed isotherms are valid only when a single binding mechanism is clearly dominant, but not in the transition region between the two regimes, which occurs around 0.2 mM. The first isotherm (BI 1) is in fact valid when individual DTAB binding clearly dominates, while the second (BI 2) is valid when hydrophobic interactions between the DTAB tails clearly dominate. In theory it would be possible to propose an interpolated isotherm to fit the transition regime around 0.2 mM. Nevertheless, even if one had a plenty of experimental points at this transition region around 0.2 mM, an interpolated isotherm would have a lot of adjustable binding parameters, such that the results returned for these parameters from the fitting would be hardly accurate.

The results of Table I show that the equilibrium binding constants of the two different mechanisms are on the same

order of magnitude, although higher for the initial individual DTAB binding.

Nevertheless, the Hill exponent obtained from the fittings suggest a completely different interpretation about the cooperativity of the two binding mechanisms. For the first one (individual binding) we obtained $n_1 \sim 1$, confirming DTAB molecules bind individually at this concentration range, i.e., independent on the previous bound surfactant molecules, and therefore the mechanism is noncooperative. Such a result is in very good agreement with the interpretation discussed in Fig. 6. On the other hand, for the second mechanism (hydrophobic interaction between the surfactant tails), the Hill exponent obtained was $n_2 \sim 3.4$, suggesting that three to four bound DTAB molecules cooperate positively, a result also in agreement with the interpretation depicted in Fig. 6. The discontinuity in the persistence length derivative at ~ 0.2 mM (see Fig. 7) arises as a result of the transition between the two DTAB binding mechanisms: individual DTAB binding for $C_T < 0.2$ mM and hydrophobic interactions between DTAB tails for $C_T > 0.2$ mM. Since cooperativity increases abruptly at the transition point (~ 0.2 mM), with the Hill exponent increasing from ~ 1 to ~ 3.4 , some type of abrupt change on the persistence length behavior is expected. Thus, the Hill exponent is the physical parameter that sets the transition between the two different binding mechanisms.

Finally, the results obtained for the local persistence length A_1 reflect the fact that the first binding mechanism tends to make the DNA more rigid, and the second one highly decreases the bending rigidity of the DNA-DTAB complexes, allowing the compaction observed in Fig. 4 for $C_T \sim 0.4$ mM.

Finally, in order to have a more precise view on the DNA compaction induced by DTAB, in Fig. 8 we plot the radius of gyration R_g of the DNA-DTAB complexes as a function of the surfactant concentration in the sample C_T . The radius of gyration was obtained from the contour and persistence length data of Figs. 4 and 5 using the equation

$$R_g = \sqrt{\frac{1}{3}AL\left(1 - \frac{3A}{L} + \dots\right)}. \quad (3)$$

Observe that for low surfactant concentrations (0 to 0.2 mM) the radius of gyration weakly increases as DTAB binds, a result correlated to the fact that the surfactant increases the persistence length of the complexes formed within this concentration range. For $C_T > 0.2$ mM, on the other hand, R_g decreases strongly as a result of DNA compaction. Such a decrease, however, is not so abrupt when compared to typical DNA condensing agents such as multivalent cations [40].

TABLE I. Binding parameters and local persistence length obtained from model fitting for each binding mechanism.

| Binding mechanism-DTAB concentration range | K (M^{-1}) | n | A_1 (nm) |
|---|------------------|---------------|--------------|
| Individual DTAB binding (0–0.2 mM) | 3700 ± 500 | 1.0 ± 0.1 | 133 ± 10 |
| Hydrophobic interaction between DTAB tails (0.2–0.4 mM) | 1100 ± 150 | 3.4 ± 0.4 | ~ 0.1 |

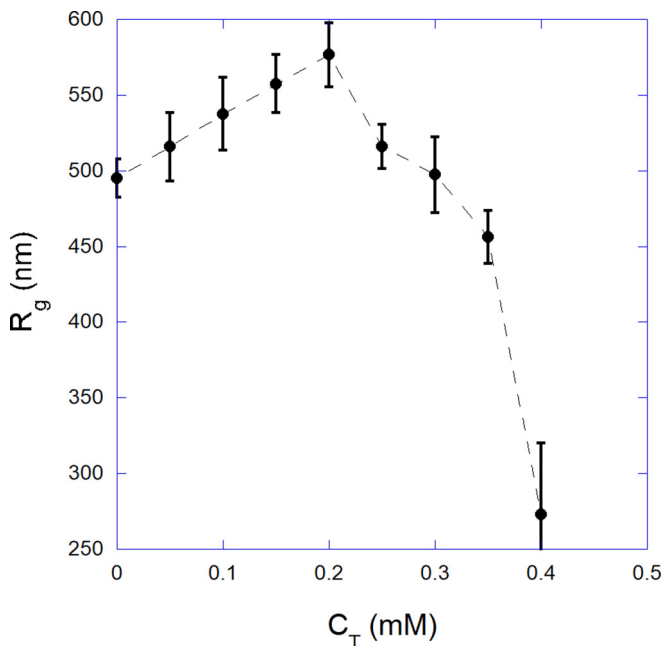


FIG. 8. Radius of gyration R_g of the DNA-DTAB complexes as a function of the surfactant concentration in the sample C_T . Observe that R_g increases until $C_T \sim 0.2$ mM and then decreases strongly as a result of DNA compaction.

C. Force clamp experiments with magnetic tweezers unveil the conditions for DTAB-induced DNA compaction

In order to investigate the role of the stretching force on the DTAB-induced DNA compaction process, here we used magnetic tweezers to apply a desired constant force on tensioned DNA molecules. In fact, magnetic tweezers can be used to maintain the biopolymer stretched at a certain constant force while introducing the surfactant in the sample chamber, allowing investigating the effects of this applied force on the DNA extension, which tends to decrease when DNA is being compacted. Such experiments complement those reported in the previous section, in which the force was varied during the assays.

We have performed the measurements at various DTAB concentrations and some values of the applied force. In summary, the conclusion was that forces as small as ~ 0.4 pN are sufficient to hinder DNA compaction under our experimental conditions. This is not in contradiction with the optical tweezers results, in which we have used forces $\lesssim 3$ pN and verified DNA compaction. The difference is that in optical tweezers assays we set the DNA-DTAB complexes free of forces after each measurement (i.e., after each force-extension curve collected). Such a procedure guarantees that DNA compaction will occur if conditions are prone to it. On the other hand, in our magnetic tweezers assays the force is always present, i.e., the DNA molecules are constantly tensioned with the desired force. Below we show some significant exemplifying results that allowed us to draw the conclusion mentioned above.

In Fig. 9 (black circles), we show a control experiment in which we maintain a bare DNA molecule stretched with a constant force of (0.40 ± 0.05) pN. The extension (end-to-end distance) of the biopolymer remains constant and equal to

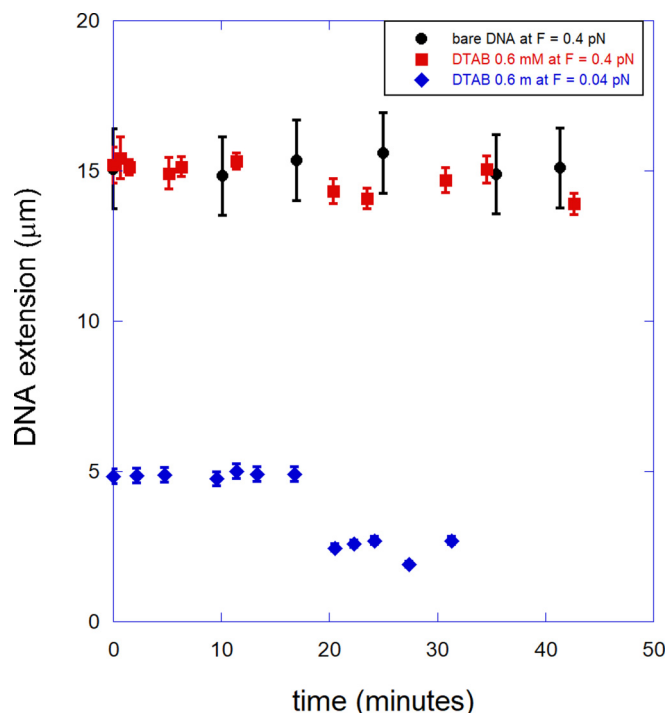


FIG. 9. Black circles: Control experiment with a bare DNA molecule stretched with a constant force of (0.40 ± 0.05) pN. Red squares: DNA-DTAB complex (DTAB at 0.6 mM) stretched with a constant force of (0.40 ± 0.05) pN. Blue diamonds: DNA-DTAB complex (DTAB at 0.6 mM) subjected to a nearly zero (~ 0.04 pN) stretching force. Such results show that even forces as small as ~ 0.4 pN are sufficient to hinder DTAB-induced DNA compaction.

(15.0 ± 1.0) μm as a function of the time, indicating that our methodology is robust and there are no drifts in the system which could lead to artifacts in the measurements. Similar experiments were performed with the same force applied on the DNA but now introducing DTAB at the beginning of the experiment (time = 0) at various concentrations in the range < 1.2 mM. In Fig. 9 (red squares), we show the particular result for 0.6 mM of DTAB. We observed that the DNA extension remains constant during the whole experiment (~ 42 min) and with the same value as the one without DTAB, showing that the surfactant does not induce any compaction on DNA when the biopolymer is tensioned with ~ 0.4 pN at the concentration range investigated ($\lesssim 1.2$ mM). In other words, no compaction occurs if forces are applied to the biopolymer maintaining its extension (~ 15 μm in the present case) close to the contour length (~ 16.5 μm for λ -DNA).

We also investigate the situation in which the biopolymer is basically free in solution, i.e., where the stretching force is completely negligible. In Fig. 9 (blue diamonds), we also show the resulting DNA extension for a constant applied force 10 times smaller, (0.040 ± 0.006) pN, i.e., nearly zero, for a DTAB concentration of 0.6 mM. Observe that there is a very significant difference from the other data: The DNA remains at the same initial extension, (4.8 ± 0.9) μm for this case, only until ~ 16 minutes after the insertion of DTAB in the working solution. Then the biopolymer is suddenly compacted to an extension of (2.5 ± 0.8) μm . This result shows that DTAB

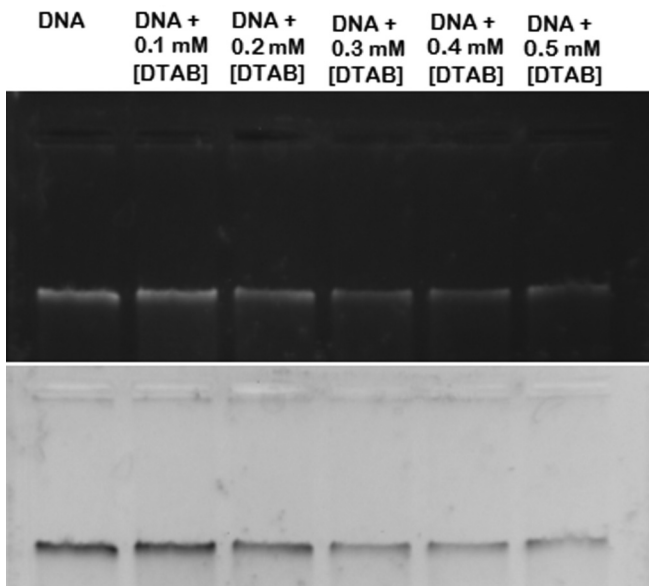


FIG. 10. Typical result of our electrophoresis assays. It can be observed that as the DTAB concentration increases, less DNA is found in the supernatant of the incubated and centrifuged samples, which confirms the effect of DTAB in compacting DNA under our experimental conditions.

compacts the DNA molecule at a concentration $C_T = 0.6$ mM if the biopolymer is basically free in solution, with a negligible stretching force applied, or, in other words, when the DNA extension is considerably smaller than the contour length. In addition, such a result allows one to estimate the timescale for the DNA-DTAB complexes to achieve chemical equilibrium, which is ~ 16 min under our experimental conditions.

D. Gel electrophoresis confirms DNA compaction by DTAB

In Fig. 10 we show a typical result of our electrophoresis assays. It can be observed that as the DTAB concentration increases, less DNA is found in the supernatant of the incubated and centrifuged samples, which were the aliquots deposited in the gel. Such a result confirms the effect of DTAB in compacting DNA and also indicates that such a compaction is not abrupt when considering a large ensemble of DNA molecules, since the brightness of the samples deposited in the different wells of the gel decreases continuously. In other words, this result shows that the number of compacted DNA molecules increases smoothly with the DTAB concentration, a conclusion that could not be obtained by performing only

single-molecule experiments such as the force spectroscopy assays presented here.

The same type of electrophoresis assay was repeated for different incubation times, from 30 min up to 10 h, and we have verified that the proportion of condensed DNA also depends on such incubation time, in addition to the DTAB concentration dependence: The longer the incubation time, more DNA condense for a given DTAB concentration. Although such a result cannot be directly compared to those obtained from our single-molecule force spectroscopy experiments, since here we are dealing with a large ensemble of molecules, it is equivalent to those obtained for DNA condensation induced by multivalent cations or neutral polymers using a similar electrophoresis assay [26].

IV. CONCLUSION

We have investigated the DNA interaction with the surfactant DTAB using three different experimental techniques: optical and magnetic tweezers and gel electrophoresis. From our optical tweezers assays, we were able to report how DTAB changes the mechanical properties of DNA on binding and the specific binding parameters of the interaction. Our results show that DTAB interacts with DNA in the concentration range of fractions of millimolar, presenting two distinct binding mechanisms: individual DTAB binding at low concentrations, followed by a strong hydrophobic interaction between the tails of the bound DTAB molecules, resulting in a DNA compaction induced by the surfactant for sufficient high concentrations. The transition between the two binding regimes is mediated by cooperativity, which increases abruptly at the transition concentration ($C_T \sim 0.2$ mM), with the Hill exponent increasing from ~ 1 to ~ 3.4 . Finally, magnetic tweezers and gel electrophoresis were used to confirm DNA compaction under our experimental conditions. These findings, along with the methodology presented here, give new insights for future studies involving surfactants and the DNA molecule.

ACKNOWLEDGMENTS

This research was funded by Conselho Nacional de Desenvolvimento Científico e Tecnológico (CNPq) Grants No. 403229/2016-2 and No. 400412/2014-4; Fundação de Amparo à Pesquisa do Estado de Minas Gerais (FAPEMIG) Grants No. 01927-16 and No. 01446-14; and Coordenação de Aperfeiçoamento de Pessoal de Nível Superior (CAPES)—Finance Code 001.

- [1] R. Dias and B. Lindman, *DNA Interactions with Polymers and Surfactants*, 1st ed. (Wiley-Interscience, New York, 2008).
- [2] K. Hayakawa, J. Santerre, and J. C. T. Kwak, The binding of cationic surfactants by dna, *Biophys. Chem.* **17**, 175 (1983).
- [3] S. Keishiro, T. Koji, and T. Noboru, Interaction between dodecyltrimethylammonium chloride and dna, *Bull. Chem. Soc. Jpn.* **60**, 43 (1987).

- [4] S. Husale, W. Grange, and M. Hegner, Interaction of cationic surfactants with dna: A single-molecule study, *Single Mol.* **3**, 91 (2002).
- [5] S. Z. Bathaie, A. A. Moosavi-Movahedi, and A. A. Saboury, Energetic and binding properties of dna upon interaction with dodecyl trimethylammonium bromide, *Nucl. Acids Res.* **27**, 1001 (1999).

- [6] P. S. Kuhn, Y. Levin, and M. C. Barbosa, Charge inversion in dna-amphiphile complexes: Possible application to gene therapy, *Physica A* **274**, 8 (1999).
- [7] M. V. Pattarkine and K. N. Ganesh, Dna-surfactant interactions: Coupled cooperativity in ligand binding leads to duplex stabilization, *Biochem. Biophys. Res. Commun.* **263**, 41 (1999).
- [8] M. Rosa, R. Dias, M. da Graca Miguel, and B. Lindman, Dna-cationic surfactant interactions are different for double and single-stranded dna, *Biomacromolecules* **6**, 2164 (2005).
- [9] K. Liu, L. Zheng, C. Ma, R. Gostl, and A. Herrmann, Dna-surfactant complexes: Self-assembly properties and applications, *Chem. Soc. Rev.* **46**, 5147 (2017).
- [10] E. Grueso and F. Sanchez, Dna-surfactant interactions: A procedure for determination group contributions, *J. Phys. Chem.* **112**, 698 (2008).
- [11] S. Bhattacharya and S. S. Mandal, Interaction of surfactants with dna. role of hydrophobicity and surface charge on intercalation and dna melting, *Biochim. Biophys. Acta* **1323**, 29 (1997).
- [12] A. Dasgupta, P. K. Das, R. S. Dias, M. G. Miguel, B. Lindman, V. M. Jadhav, M. Gnanamani, and S. Maiti, Effect of headgroup on dna-cationic surfactant interactions, *J. Phys. Chem. B* **111**, 8502 (2007).
- [13] Y. Zakrevskyy, J. Roxlau, G. Brezesinski, N. Lomadze, and S. Santer, Photosensitive surfactants: Micellization and interaction with dna, *J. Chem. Phys.* **140**, 044906 (2014).
- [14] Y. S. Mel'nikova and B. Lindman, ph-controlled dna condensation in the presence of dodecyltrimethylamine oxide, *Langmuir* **16**, 5871 (2000).
- [15] A. Gonzalez-Perez, R. S. Dias, T. Nylander, and B. Lindman, Cyclodextrin-surfactant complex: A new route in dna decompaction, *Biomacromolecules* **9**, 772 (2008).
- [16] J. P. Jost, J. Jiricny, and H. Saluz, Quantitative precipitation of short oligonucleotides with low concentrations of cetyltrimethylammonium bromide, *Nucl. Acids Res.* **17**, 2143 (1989).
- [17] T. Ahmed, A. O. Kamel, and S. D. Wettig, Interactions between dna and gemini surfactant: Impact on gene therapy: Part I, *Nanomedicine* **11**, 289 (2016).
- [18] M.-L. Ainalem, A. Bartles, J. Muck, R. S. Dias, A. M. Carnerup, D. Zink, and T. Nylander, Dna compaction induced by a cationic polymer or surfactant impact gene expression and dna degradation, *PLoS ONE* **9**, e92692 (2014).
- [19] E. Nowak, A. Wisla-Swider, G. Khachatryan, M. Fiedorowicz, and K. Danel, Possible sensor applications of selected dna-surfactant complexes, *Eur. Biophys. J.* **48**, 371 (2019).
- [20] K. R. Chaurasiya, T. Paramanathan, M. J. McCauley, and M. C. Williams, Biophysical characterization of dna binding from single molecule force measurements, *Phys. Life Rev.* **7**, 299 (2010).
- [21] M. S. Rocha, Extracting physical chemistry from mechanics: A new approach to investigate dna interactions with drugs and proteins in single molecule experiments, *Integr. Biol.* **7**, 967 (2015).
- [22] F. A. P. Crisafuli, E. B. Ramos, and M. S. Rocha, Characterizing the interaction between dna and gelred fluorescent stain, *Eur. Biophys. J.* **44**, 1 (2015).
- [23] J. F. Marko and E. D. Siggia, Stretching dna, *Macromolecules* **28**, 8759 (1995).
- [24] E. F. Silva, R. F. Bazoni, E. B. Ramos, and M. S. Rocha, Dna-doxorubicin interaction: New insights and peculiarities, *Biopolymers* **107**, e22998 (2017).
- [25] C. G. Baumann, V. A. Bloomfield, S. B. Smith, C. Bustamante, M. D. Wang, and S. M. Block, Stretching of single collapsed dna molecules, *Biophys. J.* **78**, 1965 (2000).
- [26] M. S. Rocha, A. G. Cavalcante, R. Silva, and E. B. Ramos, On the effects of intercalators in dna condensation: A force spectroscopy and gel electrophoresis study, *J. Phys. Chem. B* **118**, 4832 (2014).
- [27] C. Gosse and V. Croquette, Magnetic tweezers: Micromanipulation and force measurement at the molecular level, *Biophys. J.* **82**, 3314 (2002).
- [28] J. Lipfert, S. Klijnhout, and N. H. Dekker, Torsional sensing of small molecule binding using magnetic tweezers, *Nucl. Acids Res.* **38**, 7122 (2010).
- [29] L. D. Murphy and S. B. Zimmerman, Macromolecular crowding effects on the interaction of dna with escherichia coli dna-binding proteins: A model for bacterial nucleoid stabilization, *Biochim. Biophys. Acta* **1219**, 277 (1994).
- [30] P. Carpena, J. Aguiar, P. Bernaola-Galva, and C. C. Ruiz, Problems associated with the treatment of conductivity-concentration data in surfactant solutions: Simulations and experiments, *Langmuir* **18**, 6054 (2002).
- [31] C.-E. Lin, Determination of critical micelle concentration of surfactants by capillary electrophoresis, *J. Chromat. A* **1037**, 467 (2004).
- [32] V. A. Bloomfield, Dna condensation by multivalent cations, *Biopolymers* **44**, 269 (1997).
- [33] V. A. Bloomfield, Dna condensation, *Curr. Opin. Struct. Biol.* **6**, 334 (1996).
- [34] K. Yoshikawa, M. Takahashi, V. V. Vasilevskaya, and A. R. Khokhlov, Large Discrete Transition in a Single DNA Molecule Appears Continuous in the Ensemble, *Phys. Rev. Lett.* **76**, 3029 (1996).
- [35] C. H. M. Lima, G. O. Almeida, and M. S. Rocha, A cooperative transition from the semi-flexible to the flexible regime of polymer elasticity: Mitoxantrone-induced dna condensation, *Biochim. Biophys. Acta* **1862**, 1107 (2018).
- [36] C. H. M. Lima, J. M. C. Jr, R. M. de Oliveira, and M. S. Rocha, Pixantrone anticancer drug as a dna ligand: Depicting the mechanism of action at single molecule level, *Eur. Phys. J. E* **42**, 130 (2019).
- [37] I. Rouzina and V. A. Bloomfield, Dna bending by small, mobile multivalent cations, *Biophys. J.* **74**, 3152 (1998).
- [38] G. S. Manning, The persistence length of dna is reached from the persistence length of its null isomer through an internal electrostatic stretching force, *Biophys. J.* **91**, 3607 (2006).
- [39] L. Siman, I. S. S. Carrasco, J. K. L. da Silva, M. C. de Oliveira, M. S. Rocha, and O. N. Mesquita, Quantitative Assessment of the Interplay Between DNA-Elasticity and Cooperative Binding of Ligands, *Phys. Rev. Lett.* **109**, 248103 (2012).
- [40] I. S. S. Carrasco, F. M. Bastos, M. L. Munford, E. B. Ramos, and M. S. Rocha, Atomic force microscopy of spermidine-induced dna condensates on silicon surfaces, *Mat. Sci. Eng. C* **32**, 36 (2012).